COMPUTATIONAL ANALYSIS OF THE TUBULAR HEAT EXCHANGER OF AN INTEGRATED ENERGY GENERATION SYSTEM USING A SOLAR STIRLING ENGINE

Dan-Adrian MOCANU[1], Viorel BĂDESCU[2], Elena CARCADEA[3], ADRIAN ARMEANU[4]

An investigation of a tubular heat exchanger from an integrated cogeneration system that includes a parabolic concentrator based on a solar Stirling alpha engine is presented. The influence of the solar radiation intensity on the temperature variation of the working fluid (He) and stainless steel pipe walls is established by numerical simulations. Ansys Fluent software has been used for the computational analysis and the results obtained related to the temperature and efficiency are presented. In the case of the biggest solar radiation intensity used (1300 W/m^2), which corresponds to a very hot day, the maximum working environment temperature reaches 901 K, which is below the maximum temperature allowed for the stainless stell pipes to mantain mechanical properties and have a safe operation (923 K). An insight into tubular heat exchanger behavior at changing one operating parameter is given.

Keywords: alpha Stirling, integrated solar power, parabolic concentrator, cogeneration process, tubular heat exchanger.

1. Introduction

Energy generating systems based on parabolic concentrator and Stirling engine are a viable solution for cogeneration in a world in which the demand for cheap and clean energy is increasing every day. Currently, fossil fuels (coal, oil and natural gases) provide 80% of the electricity needed. It is therefore necessary to find alternatives, given the rapid depletion of the coal in 102 years, of the natural gases in 32 years and oil in 30 years [1].

[1] Ph.D Student Eng., National R&D Institute for Cryogenics and Isotopic Technologies - ICSI Rm. Valcea, e-mail: dan.mocanu@icsi.ro
[2] Prof., Department of Engineering Thermodynamics, University POLITEHNICA of Bucharest, Romania , e-mail: badescu@theta.termo.pub.ro;
[3] Ph.D Mat., National R&D Institute for Cryogenics and Isotopic Technologies - ICSI Rm. Valcea, e-mail: elena.carcadea@icsi.ro;
[4] Ph.D Student Eng., National R&D Institute for Cryogenics and Isotopic Technologies - ICSI Rm. Valcea, e-mail: adrian.armeanu@icsi.ro.

Since 1816, when the Stirling engine has been invented and up to now it has had a number of uses, from replacing the internal combustion systems to portable and mobile applications. Several studies have been done for investigating experimentally and theoretically the cold, hot and regenerator zones of the Stirling engines.

An important step in these investigations was made by Gustav Schimidt [5] who ideally treated the analyzed situations using algebraic analysis equations for the studied models. Taking into account the degree of model complexity, Martini [6] classified the approaches as 1st, 2nd and 3rd order, and later added the fourth degree model [7]. A first approach of characterizing and establishing the mathematical model was that of Beale [8], which has been developed and parametrized by West [9].

Over time, analytical methods are developed using differential equations, the models being divided according to Urieli-Berchowitz [10] into four main categories: isothermal, adiabatic, semi-adiabatic and quasi-adiabatic approaches. The most important contribution in the development of the second order models comes from Makhkamov and Ingham [11]. Starting with third order models more advanced algorithms based on finite element methods have been used to evaluate the Stirling engines performances. Computational Fluid Dynamics (CFD) software such as: GLIMPS third-order nodal analysis model [12] or SAGE [13] have been used by NASA in order to investigate the performance of Stirling engines. At present, among the intensively used software for fluid dynamics investigations mention ANSYS Multiphysics Fluent needed to investigate the heat and mass transfer taking place in Stirling engine [14,15], and COMSOL Multiphysics [16] needed to optimize the Stirling engine by parametrical studies.

There are several studies that investigates by CFD analysis the optimization design of a Stirling engine [17], the losses due to the complex mechanism of the Stirling engine, especially due to heat transfer [18] or the behaviour of the helium working fluids used in the heat exchangers [19]. Other research studies the spinning, yield and losses of the Stirling engine regenerator [20]. El-Ehwany studies in his work the fluid behaviour in a 10kW Stirling Solo161 engine, using a 3D software from the Lithuanian Institute for Energy. The energy source in this case is biomass [21]. Solomon and Qui in [22] thermodynamically analyze a tube heat exchanger of 4 mm with interior of 2 mm using Ansys FLUENT software based on finite volume method for investigating fluid flow and heat transfer through the walls of the tubular cooling exchanger.

The present work investigates the effects of the solar radiation for the optimization of a tubular heat exchanger (temperature, efficiency) and the results are presented as profiles and graphs for the important variables used to analyze the optimum values required by the operation.

2. System investigated

The use of an ecological power generation system based on renewable energy sources, which are virtually inexhaustible, becomes a necessity in a world facing several challenges: from fossil fuels depletion to CO_2 reduction. Such systems employ a parabolic solar concentrators based on Stirling engines. The system investigated in the present paper is composed of:

- A solar concentrator consisting of 168 mirrors with a surface of 59 m^2 mounted on a central pillar, powered by two gearmotors that perform the movements on azimuth and elevation;
- A power conversion unit based on a Stirling alpha engine, model V183 modified by Tedom, which converts solar energy into mechanical energy that drives an electric generator, resulting in electricity and heat in cogeneration.

The components of the system investigated are shown in the Figs. 1 and 2:

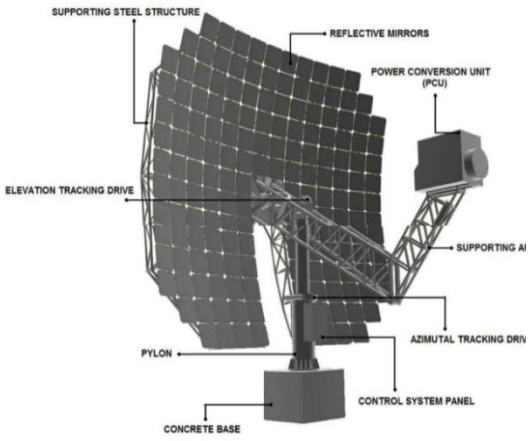

Fig. 1. Dish-Stirling system components [2]

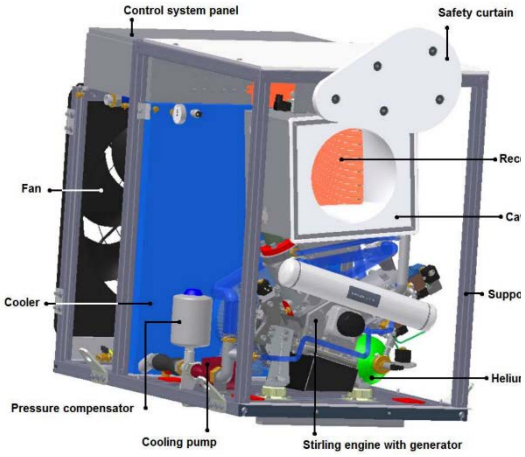

Fig. 2. Power Conversion Unit with heat Stirling engine [3]

Located in the focal point is the thermal energy production unit based on a Stirling engine, operating an electric generator and a secondary exchanger with water and 50% ethylene glycol as working fluid.

According to the manual provided by Concentrating System Ltd. Strojirny Bohdalice [2], the system allows the functioning in cogeneration, regardless of the season, in the conditions of exposure to solar radiation.

A key element that determines the system's efficiency is the primary heat exchanger (hot bulb), its investigation having the following stages: an analysis of its geometry for establishing the constructive changes necessary for the optimization; the geometry generation using a CAD software; the generation of

mesh and setting the boundary conditions, the computational analysis using ANSYS Fluent software, followed by the interpretation of results and drawing some conclusions.

2.1 Presentation of the tubular heat exchanger (hot bulb)

The positioning of the tubular heat exchanger (the hot bulb - the primary exchanger) is in the focal point of the solar concentrator, in the reflected solar radiation convergence zone, being very important to obtain a maximum efficiency of the radiant flux transmitted to the working fluid, He. It is also important that the focus area overlaps on a larger surface of the hot bulb. A front view of the Stirling engine primary exchanger is presented in Fig. 3.

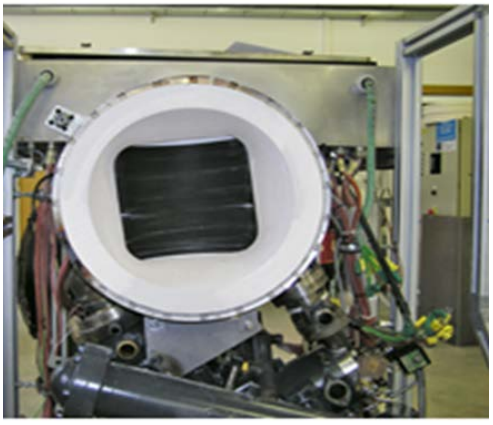

Fig. 3 Front view of the Stirling engine primary exchanger [3]

2.2 Designing the geometry of the tubular heat exchanger

The tubular heat exchanger has two side-parallel piping tanks connected by a pipe bundle. The overall dimensions of the heat exchanger are 270 mm x 350 mm x 63 mm. The slit exposed to the solar radiation is 260 x 240 (L x H), with a beam of 80 pipes. Fig. 4 presents the drawing of this primary heat exchanger (hot bulb), the Solidworks 2018 CAD software being used to generate the geometry. The components of the heat exchanger are two capillary Ø3 type pipes with a thickness of 0.5 mm and different lengths, respectively 316 mm and 332 mm. Also, the tungsten inert gas (TIG) welding was used to achieve this assembly by alternating the two types of pipes, obtaining an interstice of 0.1 mm between capillaries, thus maximizing the loss of radiant flux reflected in the focal point where the primary heat exchanger is located.

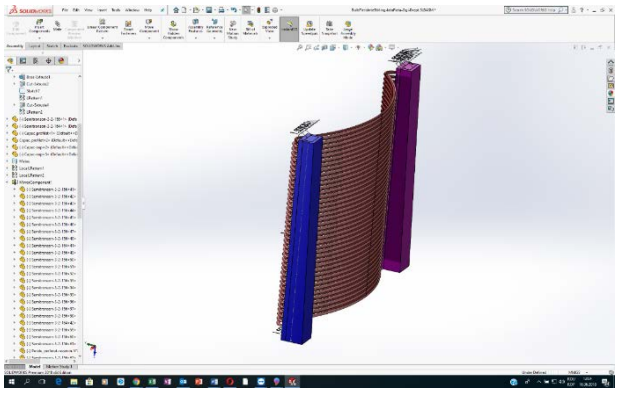

Fig. 4. Tubular heat exchanger drawing

The primary heat exchanger is made of refractory austenitic steel, brand 314 (1.4841: X15CrNiSi 25), due to high temperatures for operation, respectively 700 – 750 ^{0}C at a radiant flux of 1000-1250 W/m^2. In order to protect it from high solar radiation there is a curtain that closes automatically when the sensors record temperatures higher than the temperatures at which the material would lose the mechanical stability. This protection is achieved by the automation of the Stirling engine. The volume of the primary heat exchanger is calculated below by taking into acount the external and internal diameters of the capillary pipes as 3 and 2 mm respectively*:*

Capillary data 316	*Capillary data 332*
- $L_{desf\ 316}$=372 mm; -Interior volume: $\frac{\pi \cdot D_{int} \cdot L_{desf\ 316}}{4} = \frac{\pi \cdot 4 \cdot 372}{4} = 1168\,\text{m}^3$ (1) - V_{cap316} = 1168 mm^3; - $V_{tot\ cap316} = V_{cap316} \cdot 40 = 1168 \cdot 40 = 46723$ mm^3	- $L_{desf\ 332}$=392 mm; - Interior volume: $\frac{\pi \cdot D_{int} \cdot L_{desf\ 392}}{4} = \frac{\pi \cdot 4 \cdot 392}{4} = 1230.88\,\text{m}^3$ (2) - V_{cap332} = 1230.88 mm^3; - $V_{tot\ cap332} = V_{cap332} \cdot 40 = 1230.88 \cdot 40 = 49235$ mm^3

$V_{tot\ schimb} = V_{tot\ cap316} + V_{tot\ cap332} = 46723 + 49235 = 95958$ mm^3.
Therefore, the primary exchanger has a total volume of 96 cm^3.

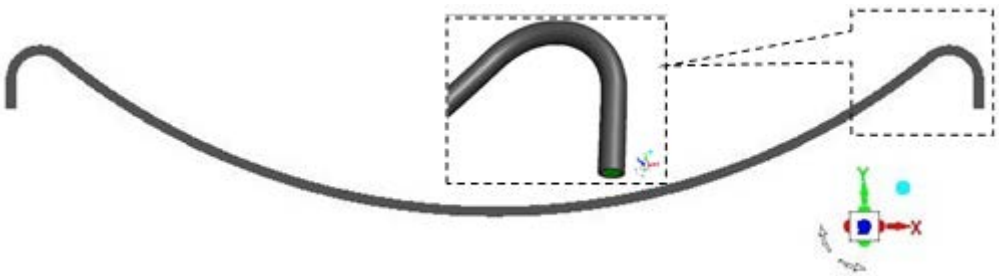

Fig. 5. Capillary heat exchanger

Another important parameter in our investigation is the concetration factor for the primary heat exchanger (hot bulb) of the Stirling engine.

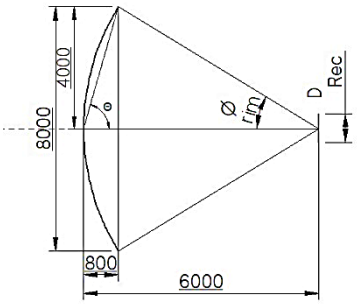

Fig. 6. Solar concentrator geometry

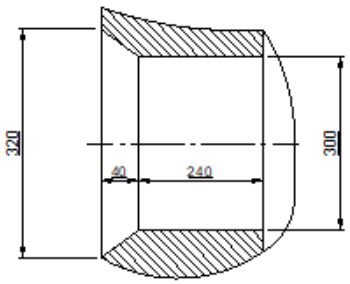

Fig. 7. Receptor geometry

The size of the receiver`s aperture allows the collection of focused energy for transmitting the heat to the primary exchanger, which further transmits the heat to the working fluid. The concentration factor *C* is defined as the ratio between the concentrator's aperture area, A_{Con} and the receptor's aperture area, A_{Rec}, acording to:

$$C = \frac{A_{Con}}{A_{Rec}} \tag{3}$$

where A_{Con} is made of 168 parabolic mirrors, each with a size of 594 x 594 x 31 mm, with a reflexive high-yield silver based layer mounted on durable glass, providing a total reflective surface of 59.3 m^2 and a reflection degree over 95%.

This results in a concentration factor:

$$C = \frac{A_{Con}}{A_{Rec}} = \frac{59.3}{0.24 \cdot 0.26} = 950 \tag{4}$$

$\eta = 0.95$;

n = 40+40 = 80 spires.

3. Optimization of stirling engine primary exchanger by simulations

The CFD analysis for heat and mass transfer of the heat exchanger was based on ANSYS Fluent Software [4]. The Stirling solar engine investigated is an alpha-modified model SB-Tedom V183 acting on one side of the piston and coupled with an electric generator. The strategy for modeling the mass and heat transfer phenomena taking place within the Stirling engines is based on: designing the geometry; generating the mesh for replacing the continuum domain with a discrete domain, setting up the mathematical models, the initial and boundary

conditions; defining the materials and their specific properties (density, porosity, permeability); model initialization; solving the transport equations (continuity, moment, energy) based on the finite volume method; convergence checking and results displaying for analyzing phenomena and effect of properties variation.

3.1 Building the geometry and mesh

The geometry developed using SolidWorks was exported as .stp file and was imported into the Gambit software, a pre-processing software used to generate geometry mesh. To obtain accurate results a refined grid mesh is necessary to ensures the independence of the solution to the grid, usually resulting in a large number of volumes. Using a small number of volumes or meshing nodes leads to significant differences between the discrete and the continuous solutions. The geometry and the mesh developed are presented in Fig. 8.

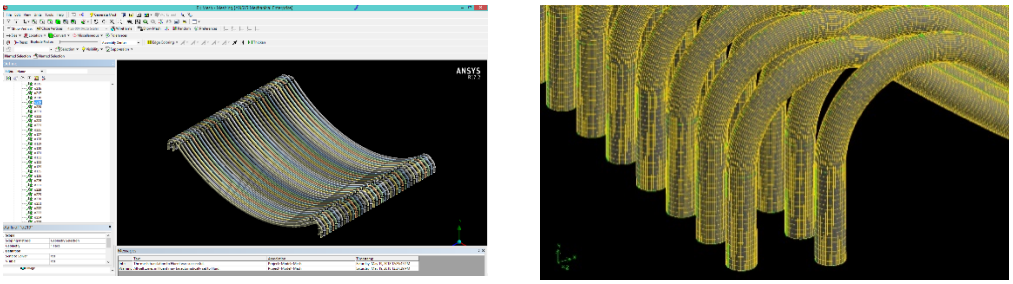

Fig. 8. Imported and discretized geometry with Workbench-Fluent

Once the mesh of the geometry is exported, it will be used in the numerical modeling with ANSYS Fluent software. As a result of the discretised geometry, a mesh with 135.000 cells per pipe and 10.800.000 cells for the 80 pipes was obtained.

3.2 Establishing the required model. Modeling.

The model used as the appropriate solution for our investigation is the Roseland model. The radiative heat flux (q_r) in a gray medium according to [4] is given by the following equation:

$$q_r = -\Gamma \nabla G \tag{5}$$

where G is the incident radiation and the parameter Γ, used for simplification, has the expression:

$$\Gamma = \frac{1}{\left[3(a+\sigma_s)-C\cdot\sigma_s\right]} \tag{6}$$

where a is the absorption coefficient, σ_s is the scattering coefficient and C is the linear-anisotropic phase function coefficient. Value of C ranges from –1 to 1, a

positive value indicates that more radiant energy is scattered forward than backward, and a negative value means that more radiant energy is scattered backward than forward [4]. A zero value defines isotropic scattering. This parameter is zero by default and is modified only if the anisotropic scattering behavior of the material used is certain.

The Rosseland radiation model assumes that the intensity is the black-body intensity at the gas temperature. Thus, $G = 4\sigma \cdot n^2 \cdot T^2$ where n is the refractive index, and substituting this value into equation (5) the following formula is obtained:

$$q_r = -16 \cdot \sigma \cdot \Gamma \cdot n^2 \cdot T^3 \cdot \nabla T \tag{7}$$

The numerical simulation is based on an iterative calculation process that involves solving the conservation equations for each volume in the mesh geometry. The iterative calculation process stops when the required precision is achieved. If a high accuracy is needed the convergence criterion will be less than 10^{-6}. Numerical modeling for a geometry that has a mesh with millions of computational cells takes between 5 and 10 hours even in the case of using parallel processing that reduces the computational time.

For all the simulations, a set of operating conditions has been specified in Table 1. Dirichlet boundary conditions for the mass flow rate and temperature were prescribed for the pipe inlets.

Table 1

The boundary conditions used in the model.

Parameter	Value	Unit
Mass flow rate at inlet	1×10^{-4}	kg/s
Temperature at inlet	330	K
Operating pressure	3-13	MPa
Solar radiation on external pipe wall	950-1300	W/m^2

4. Results and discussions

The simulations for a tubular heat exchanger with 80 pipes were carried out using the boundary conditions given in table 1 and properties of the pipes material (steel) and fluid used (He). The effect of solar radiation set up on external pipes walls is taken into consideration in our numerical analysis and the impact on temperature and efficiency is investigated, the results being presented as contours and graphs.

Taking into account the concentration factor, efficiency and number of capillaries calculated in section 2 and by varying the solar radiation that fluctuates

during the day and seasons we calculate the concentrated radiation on the pipes, the results being presented in Table 2.

Tabel 2

Calculation of radiated radiation on a spiral

No.	Solar radiation (W/m^2)	Concentration factor C	Concentration efficiency η	Number of capillaries n	Concentrated radiation on the pipe (W/m^2)
1.	950	950	0.95	80	10700
2.	1000	950	0.95	80	11250
3.	1050	950	0.95	80	11800
4.	1100	950	0.95	80	12375
5.	1150	950	0.95	80	12900
6.	1200	950	0.95	80	13500
7.	1245	950	0.95	80	14000
8.	1300	950	0.95	80	14625

Taking into account a intensity of the solar radiation of 1300 W/m^2, the countours of temperature in the working fluid (He) and at external surfaces of the steel pipes are presented in Figs. 10 and 11, respectively, as a result of Ansys Fluent simulations.

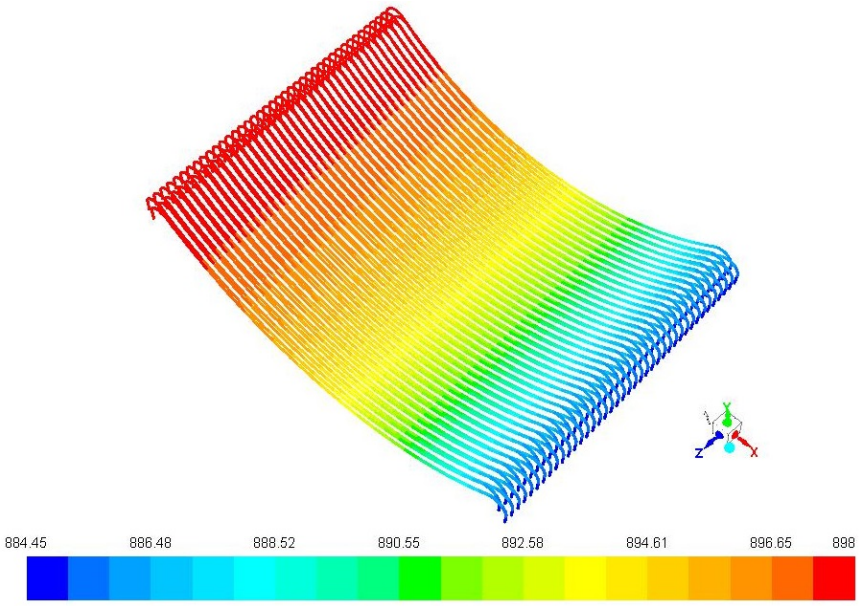

Fig. 10. Temperature of working fluid (He) for 1300 W/m^2 solar radiation intensity

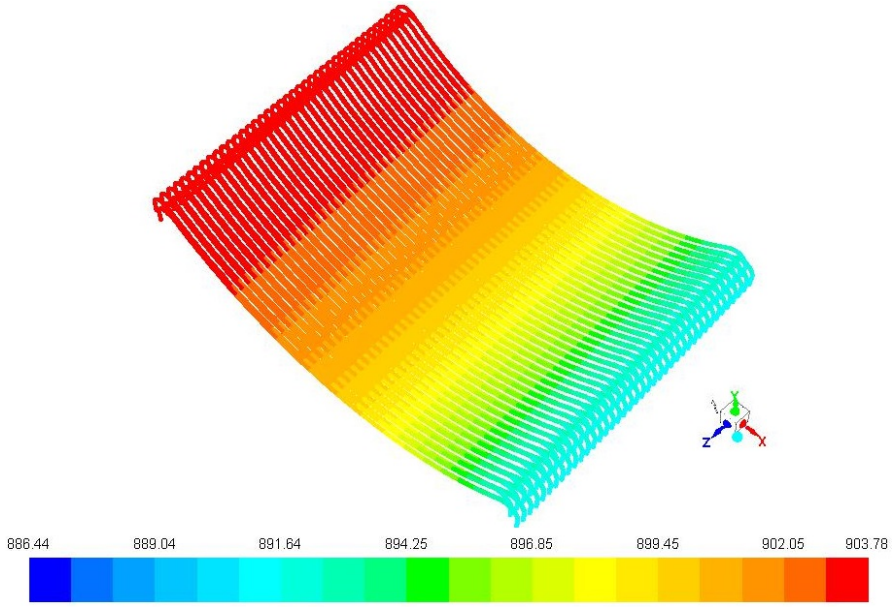

Fig. 11. Temperature of stainless steel pipes for 1300 W/m^2 solar radiation intensity

Table 3 gives the minimum and maximum temperatures obtained in the numerical simulations for each solar radiation value taken into account.

Tabel 3

Simulation results for different values of solar radiation

NO	Solar radiation	Cold source temperature	Wall temperature tube Stainless steel- 314		Working fluid temperature - He		Min yield	Max yield	Stirling engine efficiency
			Minimum	Maximum	Minimum	Maximum			
-	-	T_R	$T_{T_{in}}$	$T_{T_{out}}$	$T_{He_{in}}$	$T_{He_{out}}$	$\frac{T_{He_{in}}}{T_{T_{in}}}$	$\frac{T_{He_{out}}}{T_{T_{out}}}$	$1-\frac{T_R}{T_C}$
-	W/m^2	K	K	K	K	K	-	-	-
1.	950	330	704	826	552	750	0.7840	0.9079	0.56
2.	1000	330	719	841	577	770	0.8025	0.9155	0.57
3.	1050	330	746	867	606	793	0.8123	0.9146	0.58
4.	1100	330	763	886	633	815	0.8296	0.9198	0.60
5.	1150	330	784	906	660	837	0.8418	0.9238	0.61
6.	1200	330	800	938	687	876	0.8587	0.9339	0.62
7.	1250	330	818	940	710	880	0,8679	0,9361	0.63
8.	1300	330	847	960	742	901	0.8760	0.9376	0.63

It is very important to obtain a maximum efficiency of the radiant flux transmitted to the working fluid, He. In Fig. 12 are presented the minimum and maximum thermal transfer efficiencies obtained from CFD simulations, and also

the Stirling engine efficiency while varying the solar radiation. It can be noticed that the thermal efficiency of the tubular heat exchanger is increasing with the increase of solar radiation intensity and for the Stirling engine efficiency a maximum value is obtained for solar radiation intensity higher than 1200 W/m^2.

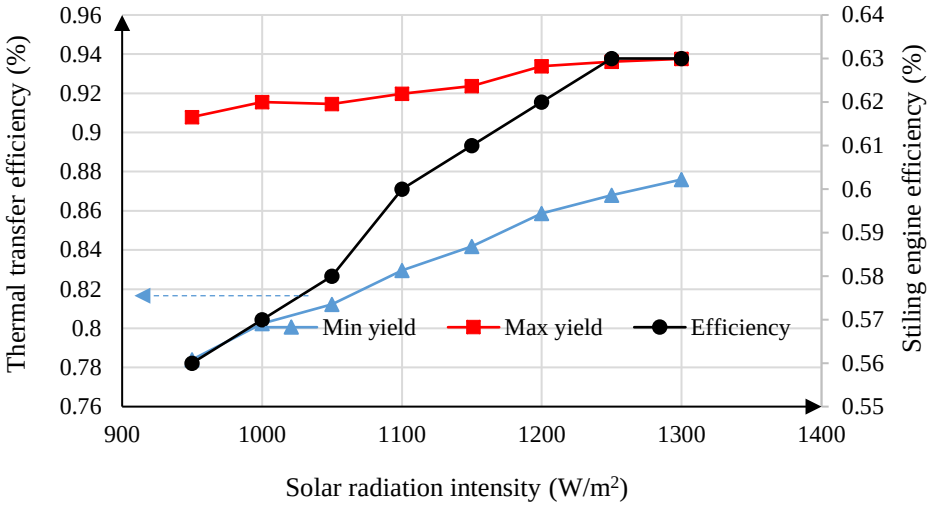

Fig. 12. Maximum efficiency for variation of solar radiation

5. Conclusions

The behavior of the Stirling engine primary heat exchanger (bulb) at changing the solar radiation intensity was investigated in this paper. First, the 3D geometry, mesh design and 3D computational analysis have been developed using Ansys Fluent software, followed by the calculation of some key parameters for the heat exchanger, such as: volume, concentration factor and efficiency, parameters that are used in the CFD simulations.

The influence of the solar radiation intensity on the operation of a tubular heat exchanger is given by the numerical simulations. The results, displayed as contour profiles and graphs, show the variation in temperatures and Stirling engine efficiency. It has been found that in the case of the biggest solar radiation intensity that corresponds to a very hot day (1300 W/m^2), the maximum working temperature reaches 901 K, which is below the maximum temperature allowed for mantaining the mechanical properties and safe operation of the stainless stell pipes (923 K). Also, the maximum Stirling engine efficiency, 63%, is reached for solar radiation intensity higher than 1200 W/m^2.

The study was intended to give an insight on the tubular heat exchanger behavior at changing one operating parameter and future work will be devoted to the geometry and design parameters optimization.

REFERENCES

[1]. *S. Shafiee, E. Topal,* "When will fossil fuel reserves be diminished?" in Energy Policy **vol. 37**, 2009, pp. 181–189.

[2]. ***Manual Instruction – V1.0 - Sunflower 35 CONCENTRATION SOLAR PLANT-STROJÍRNY BOHDALICE, a.s., November 30, 2014.

[3]. www.concentrating.eu.

[4]. http://www.ansys.com/Products/Fluids/ANSYS-Fluent.

[5]. *G. Schmidt*, "Classical analysis of operation of Stirling engine", A report published in German Engineering Union (Original German), **vol. XV**, 1871, pp. 1–12.

[6]. *W. Martini*, Stirling engine design manual, 1983. DOE/NASA/3194-1, NASA CR-168088.

[7]. *R. W. Dyson, S. D. Wilson, R. C. Tew*, "Review of computational Stirling analysis methods", National aeronautics and space administration. (No. AIAA–2004–5582); 2004.

[8]. *W. T. Beale, J. G. Wood, B. F. Chagnot*, "Stirling engine for developing countries" in Am Inst. Aeron Astron, **vol. 809399**, 1980, pp.1971–1975.

[9]. *C. D. West*, A fluidyne STIRLING engine. Report no AERE-R 6776, Harwell University; 1981.

[10]. *I Urieli, DM Berchowitz*, Stirling cycle engine analysis. Taylor & Francis; 1984.

[11]. *Kh. Kh. Makhkamov, D. B. Ingham*, "Analysis of the Working Process and Mechanical Losses in a Stirling Engine for a Solar Power Unit", Journal of Solar Energy Engineering, **vol. 121**, 1999, pp. 121-127.

[12]. *D. Gedeon*, "A Globally-Implicit Stirling Cycle Simulation" 21st Intersociety Energy Conversion Engineering Conference, American Chemical Society, **vol. 1**, 1986, pp. 550-554.

[13]. *D. Gedeon*, Sage user's guide. Sage v11 Edition, 2016, http://www.sageofathens.com/ Documents /SageStlxHyperlinked.pdf.

[14]. *T. Alexakis*, CFD modelling of Stirling engines with complex design topologies. PhD Thesis, Northumbria University, 2013.

[15]. *S. A. El-Ghafour, M. El-Ghandour, N. N. Mikhael*, "Three-dimensional computational fluid dynamics simulation of Stirling engine" in Energy Conversion and Management, **vol. 180**, 2019, pp. 533–549.

[16]. *A. K. Almajri, S. Mahmoud, R. Al-Dadah*, "Modelling and parametric study of an efficient Alpha type Stirling engine performance based on 3D CFD analysis" in Energy Conversion and Management, **vol. 145**, 2017, pp. 93–106.

[17]. *G. Xiao, U. Sultan, M. Ni, H. Peng, X. Zhou, S. Wang, Z. Luo*, "Design optimization with computational fluid dynamic analysis of b-type Stirling engine" in Applied Thermal Engineering, **vol. 113**, 2017, pp. 87–102.

[18]. *A.J. Organ*, Stirling Cycle Engines: Inner Workings and Design, John Wiley & Sons, 2013.

[19]. *J. Bert, D. Chrenko, T. Sophy, L.L. Moyne, F. Sirot*, "Simulation experimental validation and kinematic optimization of a Stirling engine using air and helium" in Energy, **vol. 78**, 2014, pp. 701–712.

[20]. *I. Tlili, Y. Timoumi, S.B. Nasrallah*, "Thermodynamic analysis of the Stirling heat with regenerative losses and internal irreversibilities" in International Journal of Engine Research, **vol. 9**, no. 1, 2008, pp. 45-56.

[21]. *A.A. El-Ehwany, G.M. Hennes, E.I. Eid, E.A. El-Kenany*, "Development of the performance of an alpha-type heat engine by using elbow-bend transposed-fluids heat exchanger as a heater and a cooler" in Energy Conversion and Management, **vol. 52**, 2011, pp. 1010–1019.

[22]. *Laura Solomon, S. Qiu*, "Computational analysis of external heat transfer for a tubular Stirling convertor" in Applied Thermal Engineering, **vol. 137**, 2018, pp. 134–141.